

Ferromagnetism and Metamagnetism in Copper-doped Germanium Clathrate

Yang Li, Weiping Gou, Ji Chi, and Joseph H. Ross, Jr.
Department of Physics, Texas A&M University, College Station, TX 77843-4242
(Dated: November 20, 2018)

Cu-doped type-I germanium clathrate can exhibit dilute magnetism, including ferromagnetism, antiferromagnetism, and metamagnetic transitions up to 90 K. ^{63}Cu NMR measurements confirm that these transitions are due to a dilute composition of magnetic defects coupled by conduction electrons, behavior similar to that of magnetic semiconductors. Magnetic measurements indicate localized magnetic moments, attributed to clusters of magnetic ions, with competition between ferromagnetic and antiferromagnetic exchange, and also indications of glassy behavior in the ferromagnetic phase. NMR Knight shifts and relaxation times show that the conduction band is metallic with a large Korringa ratio. Comparison to a mean-field theory for the ordering behavior gives a good accounting for the ferromagnetic transition.

Magnetic semiconductors have been the focus of renewed interest, due in part to the potential for spin injection in semiconductor electronics [1, 2]. There have been a number of recent successes in the magnetic doping of semiconductors, for instance GaAs can be doped out of equilibrium with Mn using low-temperature molecular-beam epitaxy [1] to yield transition temperatures reported as high as 160 K. Ferromagnetism in these materials is due to the combined action of magnetic ions and a polarized conduction band of itinerant electrons. The magnetic ground state can be complex due to the competition between locally ferromagnetic and antiferromagnetic exchange couplings, as well as the positional disorder of dopant atoms [3, 4, 5, 6]. Thus, the nature of the ordering process is of fundamental interest.

The clathrate structure is one way to stabilize magnetic ions in group-IV semiconductors. Clathrates [7] feature fullerene-type cages in a crystalline framework enclosing electron-donating ions such as Na and Ba. The electron-donors can be balanced by electron-deficient transition-metals substituted onto the framework [8], to produce materials ranging from semiconducting to metallic. This is in contrast to GaAs:Mn, where Mn ions produce strong hole-doping. The open clathrate crystal structure can lead to flat electron band features, and therefore sharp density of states peaks [9], which enhance the tendency toward magnetism and superconductivity. In this letter, we describe the magnetism of a dilute magnetic Ge clathrate exhibiting competition between ferromagnetic and antiferromagnetic interactions.

Group-IV clathrates have a wide variety of electronic properties. The observations of superconductivity [10] and “electron crystal, phonon glass” behavior [11] in Ge and Si clathrates have sparked particular interest. The cages can be vacated, leaving a new elemental form of Si [12], and there is a possibility that these materials may grow epitaxially on a diamond substrate [13]. Ferromagnetism has been observed in Mn-substituted Ge clathrate [14] and in clathrates with Eu ions in the cages [15]. Here we show that dilute Cu-doped Ge clathrates can exhibit metamagnetism and ferromagnetism, medi-

ated by the conduction electrons.

For sample preparation, ingots of $\text{Ba}_8\text{Cu}_x\text{Ge}_{46-x}$, were induction melted, then reacted for 3 days at 950°C and 4 days at 700°C in evacuated ampoules. Cu substitutes on the 46 site/cell Ge framework in this case [7]. Diffraction and microprobe analysis [16] have shown that the type-I clathrate of approximate composition $\text{Ba}_8\text{Cu}_5\text{Ge}_{40}$ is stabilized by a Zintl mechanism, with vacancies appearing spontaneously to maintain the electron count. By changing the starting material, the Cu content varies over a narrow range. The samples described here, denoted Cu2 and Cu6, had starting compositions $x = 2$ and 6, respectively. Microprobe analysis showed that in the Cu6 sample, the clathrate contains 8% additional Cu. In addition, this sample contains a small amount of Ge_3Cu_5 phase intermixed with the clathrate, while the Cu2 sample has no other Cu-containing phases [16].

Fig. 1 shows magnetization (M) curves for the Cu6 sample, obtained using a Quantum Design SQUID magnetometer. Typical ferromagnetic hysteresis is seen at 2 K, going over to a diamagnetic slope at high fields as the ferromagnetic response becomes saturated, showing the underlying diamagnetism of the lattice. At intermediate temperatures the response is metamagnetic, shown in the insets to Fig. 1 as a field-induced transition to ferromagnetic order. The transition is first-order at 60 K, then disappears at higher temperatures.

M vs. T has been plotted in Fig. 2. In low fields there is a feature at 90 K, associated with an antiferromagnetic transition for the Cu6 sample, since the sample remains diamagnetic below this temperature. The field-cooled (FC) curve has a further cusp at 12 K, associated with a driven ferromagnetic response of the conduction electrons. In larger fields, the 90 K feature becomes less distinct and eventually disappears, as shown for 4 T applied field. A Curie law fits the 4 T data between 55 K and 400 K (solid curve), with $T_c = 34$ K.

The 0.1 T zero-field-cooled (ZFC) and FC data in Fig. 2 show irreversibility below 32 K. Furthermore, the data cross, behavior which has been observed in entrant spin glass systems [17, 18], in which a ferromag-

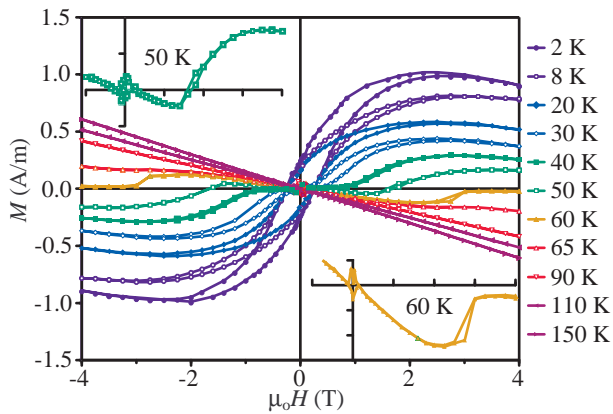


FIG. 1: Magnetization vs. field for Cu6 sample. The labeled temperatures have the same vertical ordering as the curves on the right side of the figure. Expanded views for 50 K and 60 K are inset, showing the metamagnetic response at these temperatures.

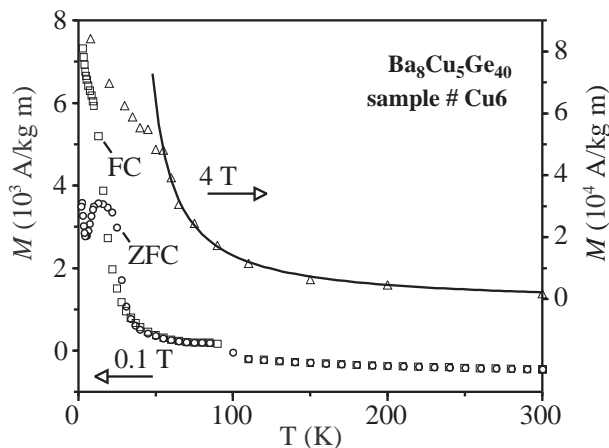


FIG. 2: Magnetization vs. temperature for Cu-doped clathrate. 0.1 T data are field-cooled (FC, squares) and zero-field cooled (ZFC, circles) as indicated. Solid curve is Curie-law fit to 4 T data.

netic state disorders at low temperatures due to random antiferromagnetic bonds, and field-alignment locks some regions into reverse-orientation, reducing the net M .

The Cu2 sample also exhibits low-temperature ferromagnetism. Spontaneous magnetization appears near 10 K, with a saturation moment similar to that of Cu6. However, no metamagnetism was observed for the Cu2 sample, indicating the concentration-dependent nature of this behavior.

Results for Cu6 are summarized in the phase diagram of Fig. 3. Circles are metamagnetic transitions identified from slope changes or jumps in magnetization (Fig. 1). The enclosed phase is antiferromagnetic. The metamagnetic transition changes from second-order to first order between 50 K and 60 K, as seen from the insets to Fig. 1. Thus we have plotted a tri-critical point be-

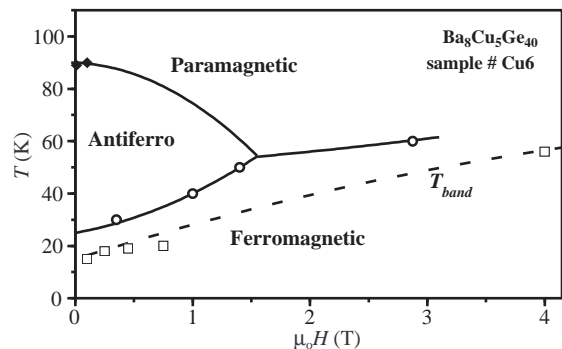


FIG. 3: Phase diagram for the metamagnetic Cu6 sample, with an approximate rendering of the phase boundaries. T_{band} is described in the text.

tween these temperatures. The first-order curve ends in a critical point beyond which the paramagnetic state goes continuously into the ferromagnetic state, shown by the unbroken Curie behavior seen in 4 T (Fig. 2). This phase diagram is quite similar to that of NdRu_2Ge_2 [19]. Metamagnetism is not uncommon in such rare-earth intermetallics due to frustrated ferromagnetic and antiferromagnetic coupling of rare earth moments, mediated by the conduction electrons. Here the local moments are due to the random distribution of Cu on Ge framework sites in the clathrate.

The square symbols in Fig. 3 identify further slope changes in M vs. T , for example the 4 T data departing from the Curie fit in Fig. 2). At low fields these appear below the metamagnetic line. As shown below, this feature is consistent with the saturation of the band electrons, thus the label T_{band} .

Since M approaches the lattice diamagnetic slope at high fields (Fig. 1), we measured the 400 K response in order to establish this slope, and thus determine the low-temperature saturation moment, M_s . With an applied field of 7 T, we obtained $M_s = 0.085\mu_B$ per cell in the Cu6 sample. Since $M_s = gJ\mu_B n$, and the Curie law is $\chi = n\mu_0\mu_B^2 p_{eff}^2 / 3k(T - T_c)$, the measurements may be used to evaluate n , the spin density, and $p_{eff} = g\sqrt{J(J+1)}$, the local moment. In our case J is unknown, however assuming $J = 1/2$, the 4 T Curie fit (Fig. 2) gives $n = 0.023$ per cell and $p_{eff} = 6.2\mu_B$. Alternatively, $J = 5/2$ gives $n = 0.011$ per cell and $p_{eff} = 9.2\mu_B$, in either case a dilute set of moments

In type-I Ge clathrates, transition metal atoms generally substitute on the 6c crystallographic site, 6 per unit cell among the 46 framework sites [8]. Using NMR as a local probe of the Cu sites, we find that the main line consists of non-magnetic Cu in a high-symmetry environment, consistent with occupation of the 6c site. The moments of 6.2 or $9.2\mu_B$ are too large to be single ions, and are presumed associated with composite clusters of neighboring atoms, possibly centered upon wrong-site Cu

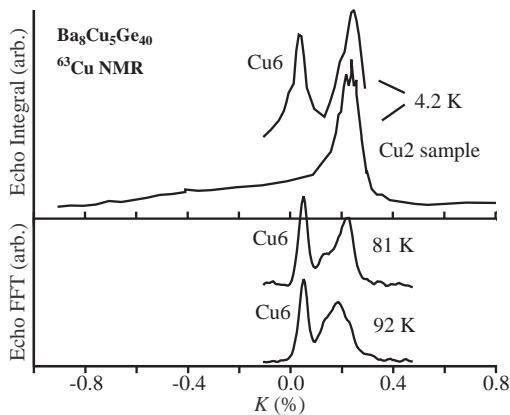


FIG. 4: ^{63}Cu NMR spectra for the two samples. 4.2 K data measured via echo integration; lower two traces measured via small tip-angle echo FFT. Data offset vertically for clarity.

atoms. Competition between antiferromagnetic superexchange and ferromagnetic double exchange is well known for magnetic semiconductors [5, 20], and this can explain the metamagnetic behavior observed here: competing internal interactions in the clusters, in addition to the RKKY interaction between clusters, can cause a switching in the magnetic alignment.

^{63}Cu NMR confirms that the dilute magnetism is intrinsic to the clathrate. Data were obtained in a fixed applied field of 9 T. Above 4 K, data were obtained by FFT of small-tip-angle spin echoes, allowing the frequency range to be extended. Fig. 4 shows NMR lineshapes, on a Knight shift (K) scale based on an aqueous $^{27}\text{AlCl}_3$ reference and published gyromagnetic ratios [21]. The peak near $K = 0.2\%$ is common to both samples, while Cu6 has an additional lower- K peak, changing little with temperature, due to the presence of Ge_3Cu_5 in that sample. A low- K tail was also seen for both samples, as shown in the 4.2 K Cu2 data. This tail can be attributed to nuclei in direct contact with magnetic sites, while the main peak is more characteristic of a non-magnetic metal: Cu metal has $K = 0.239\%$ [21], while the typical range for Cu compounds and nonmagnetic intermetallics is 0 – 0.2 %.

We attributed the low- K NMR peak to Ge_3Cu_5 since it appears only in the Cu6 sample. (Ge_3Cu_5 is apparently stabilized by the clathrate; attempts to produce this phase alone gave instead a mixture of Ge and orthorhombic GeCu_3 , with a T -independent spectrum different from those of Fig. 4.) The higher- K peak has the symmetry expected for the nearly-tetrahedral clathrate lattice. The $6c$ site has four identical nearest neighbors, and X-ray diffraction of the Cu clathrate shows the bond angles for this site to be within 0.5° of perfect tetrahedral symmetry [16]. The other framework sites also approximate a tetrahedral bonding configuration, but with somewhat more distorted bond angles and

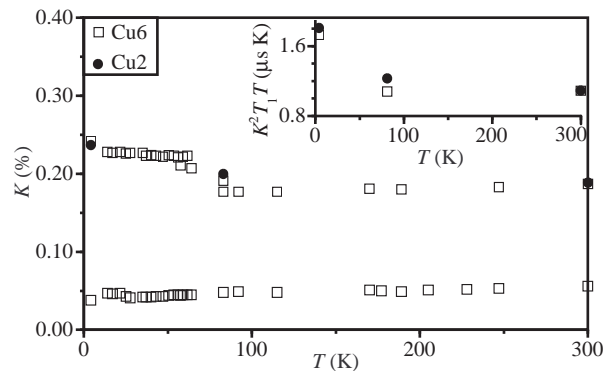


FIG. 5: ^{63}Cu NMR peak Knight shifts vs. temperature. Inset shows the $K^2 T_1 T$ product.

crystallographically inequivalent neighbors. For the $6c$ site, we expect small electric field gradients and small electric quadrupole splittings in ^{63}Cu NMR, while lower symmetry gives typically a central transition flanked by quadrupole-split satellites. The matrix elements determining the NMR pulse angles differ by a factor of two for these cases [22]. Our investigation of the pulse response showed that the lower- K Cu6 line is a central transition, corresponding to a lower-symmetry environment in the unknown Ge_3Cu_5 material. The other Cu6 line, and the corresponding line in Cu2, has little or no quadrupole splitting, characteristic of a high-symmetry environment, consistent with its assignment to Cu occupying the $6c$ site of the clathrate framework.

Fig. 5 shows K vs. T , with points representing lineshape maxima. For the clathrate $6c$ -line in both samples, K increases at low T . This increase is most prominent for the range 60 – 90 K in Cu6, and we also observed a warming/cooling hysteresis between 77 K and 90 K. Extrapolating the curve T_{band} (Fig. 3) to the 9 T field of the NMR spectrometer, we see that changes in K occur over the range where the band moment is expected to be changing most rapidly. Thus, the $6c$ resonance exhibits changes that correspond to changes in the magnetism, which we confirm to be intrinsic to the clathrate.

The NMR spin-lattice relaxation time, T_1 , follows a Korringa law in both samples, indicating the presence of a metallic conduction band. T_1 was obtained by inversion-recovery, with a fit to a single exponential recovery curve for the $6c$ site, appropriate for cases with no quadrupole splitting [22]. The product $K^2 T_1 T$ is shown in the inset of Fig. 5. For both samples, $K^2 T_1 T$ is nearly constant above 90 K, characteristic of relaxation by a metallic band [21]. The increase in $K^2 T_1 T$ at low temperatures is due almost entirely to changes in K . $K^2 T_1 T$ values are smaller than that expected for the bare nucleus, $3.8\mu\text{s K}$, which can come about if the Knight shift is a difference of terms, with the negative contribution due to core polarization, for which the hyperfine cou-

pling is negative [21]. This indicates a contribution of Cu d -electrons to the conduction band. However, the fact that the T_1 change is much smaller than that of K indicates that many of the carriers are unaffected by the transition, probably due to multiple bands crossing the Fermi surface [9].

The low- T increase in K is consistent with a band polarized in the opposite sense to the local moments, assuming that the shift is dominated by core polarization, which has negative hyperfine coupling for Cu. Using the coupling constant $H^{cp} = -12.5$ T [21], the low-temperature change in K , $+0.073$ % for Cu6, corresponds to a saturated conduction-band magnetization $M = -0.0032\mu_B$ per cell. In this calculation we assumed the band magnetization to be distributed equally among the 46 framework sites. If we also approximate by assuming that this magnetization is linear in the defect magnetization, we can use the mean-field transition temperature calculated for conduction-band-coupled localized moments [23]:

$$k_B T_c = \frac{np_{eff} J_{int}^2 \chi}{4\pi(g^* \mu_B)^2}. \quad (1)$$

Here J_{int} is the coefficient of a delta-function interaction between the local moments and the band, χ is the band susceptibility, and g^* its g -factor. Assuming the conduction electrons are uniformly polarized by the effective Zeeman field corresponding to J_{int} , we can write $M = \chi n J g J_{int} / (\mu_0 g^* \mu_B)$ for the band magnetization which we evaluated using the Knight shift. Using $J = 5/2$, $n = 1.1\%$, and $p_{eff} = 9.2$ as extracted above, $g^* = 2$, and $T_c = 12$ K, we obtain $J_{int} = 0.27$ eV nm³ and $\chi = 1.4 \times 10^{-5}$ (SI dimensionless). These are plausible values; $J_{pd} = 0.055$ eV nm³ was obtained for Mn in GaAs [23], while the χ we obtain is about one-fifth that of copper metal [21].

Since the susceptibility is in the metallic range, and the magnetic defects well separated, one might expect that spin glass ordering would result from the oscillatory RKKY interaction. However, the clathrate structure can lead to large band masses and sharp electron density of states features [9], which may enlarge the oscillation period simply by the decrease of the Fermi wavevector, or possibly by enhancing the response for $k = 0$ in the sense of a paramagnon system [24]. These features could make related clathrate systems useful for future spin-related applications.

Thus, we have shown that the Cu-doped Ge clathrate can exhibit a rich magnetic structure, including an anti-ferromagnetic phase which features a metamagnetic transition to the ground-state ferromagnetic configuration. NMR measurements confirmed this behavior to be due to a dilute set of magnetic clusters, coupled via the conduction-band electrons.

This work was supported by the Robert A. Welch

Foundation, Grant No. A-1526, and by Texas A&M University through the Telecommunications and Informatics Task Force.

-
- [1] H. Ohno, *Science* **281**, 951 (1998).
 - [2] H. Ohno, D. Chiba, F. Matsukura, T. Omiya, E. Abe, T. Dietl, Y. Ohno, and K. Ohtani, *Nature (London)* **408**, 944 (2000).
 - [3] J. Schliemann and A. H. MacDonald, *Phys. Rev. Lett.* **88**, 137201 (2002).
 - [4] G. Zaránd and B. Jankó, *Phys. Rev. Lett.* **89**, 047201 (2002).
 - [5] T. Dietl, H. Ohno, and F. Matsukura, *Phys. Rev. B* **63**, 195205 (2001).
 - [6] J. König, H.-H. Lin, and A. H. MacDonald, *Phys. Rev. Lett.* **84**, 5628 (2000).
 - [7] J. S. Kasper, P. Hagenmuller, M. Pouchard, and C. Cros, *Science* **150**, 1713 (1965).
 - [8] G. Cordier and P. Woll, *J. Less-Common Met.* **169**, 291 (1991).
 - [9] J. Gryko, P. F. McMillan, R. F. Marzke, A. P. Dodokin, A. A. Demkov, and O. F. Sankey, *Phys. Rev. B* **57**, 4172 (1998).
 - [10] H. Kawaji, H. Horie, S. Yamanaka, and M. Ishikawa, *Phys. Rev. Lett.* **74**, 1427 (1995).
 - [11] G. S. Nolas, J. L. Cohn, G. A. Slack, and S. B. Schujman, *Appl. Phys. Lett.* **73**, 178 (1998).
 - [12] J. Gryko, P. F. McMillan, R. F. Marzke, G. K. Ramachandran, D. Patton, S. K. Deb, and O. F. Sankey, *Phys. Rev. B* **62**, R7707 (2000).
 - [13] S. Munetoh, K. Moriguchi, K. Kamei, A. Shintani, and T. Motooka, *Phys. Rev. Lett.* **86**, 4879 (2001).
 - [14] T. Kawaguchi, K. Tanigaki, and M. Yasukawa, *Appl. Phys. Lett.* **77**, 3438 (2000).
 - [15] B. C. Chakoumakos, B. Sales, and D. G. Mandrus, *J. Alloy Compd.* **322**, 127 (2001).
 - [16] Y. Li, J. Chi, W. Gou, S. Khandekar, and J. H. Ross, Jr., eprint cond-mat/0210244.
 - [17] Y. Öner, C. S. Lue, J. H. Ross, Jr., K. D. D. Rathnayaka, and D. G. Naugle, *J. Appl. Phys.* **89**, 7044 (2001).
 - [18] B. R. Coles and S. B. Roy, in *Selected Topics in Magnetism*, edited by L. C. Gupta and M. S. Multani (World Scientific, Singapore, 1993), p. 363.
 - [19] D. Gignoux and D. Schmitt, in *Handbook of the Physics and Chemistry of Rare Earths*, edited by K. A. Gschneidner, Jr. and L. Eyring (Elsevier, Amsterdam, 1995), vol. 20, p. 293.
 - [20] S. Methfessel and D. C. Mattis, in *Handbuch der Physik*, edited by H. P. J. Wijn (Springer, Berlin, 1968), vol. 18, part 1.
 - [21] G. C. Carter, L. H. Bennett, and D. J. Kahan, eds., *Metallic Shifts in NMR* (Pergamon, 1977).
 - [22] O. Kanert and M. Mehring, in *NMR: Basic Principles and Progress*, edited by E. Fluck and R. Kosfeld (Springer-Verlag, New York, 1971), vol. 3, p. 1.
 - [23] T. Jungwirth, J. König, J. Sinova, and A. H. MacDonald, *Phys. Rev. B* **66**, 012402 (2002).
 - [24] T. Moriya, *Spin Fluctuations in Itinerant Electron Magnetism* (Springer, 1985).